Available at www.sciencedirect.com

ScienceDirect

journal homepage: www.elsevier.com/locate/he

On the stability of ultra-lean H_2/CO combustion in inert porous burners ☆

*M.A.A. Mendes, J.M.C. Pereira, J.C.F. Pereira**

Mechanical Engineering Department, Instituto Superior Técnico, Technical University of Lisbon, LASEF Av. Rovisco Pais 1, 1049-001, Lisbon, Portugal

ARTICLE INFO

Article history:
Received 4 January 2008
Received in revised form
8 April 2008
Accepted 8 April 2008
Available online 2 June 2008

Keywords:
Hydrogen–carbon monoxide mixtures
Syngas
Ultra-lean combustion
Porous burner
Linear stability analysis

ABSTRACT

The stability of ultra-lean H_2/CO mixtures in a porous media burner is numerically investigated. The one-dimensional model considers separated energy equations for the solid and gas phases and accounts for radiative heat transfer in the solid porous foam. A simplified reaction kinetics (two-step mechanism) was employed in order to perform a linear stability analysis. This results are used to investigate the stability of the steady solutions as a function of burning velocity and flame location. The present analysis includes the effects of H_2/CO volumetric ratio, inlet mixture temperature and equivalence ratio on the flame stability. From the linear stability results it can be concluded that the insertion of inert porous media for premixed combustion promotes the ultra-lean burning of H_2/CO mixtures.

1. Introduction

The combustion of hydrogen and carbon monoxide mixtures is getting a great deal more attention these days. With rising cost of oil there is an interest in cheaper and environmentally acceptable replacement for the oil and natural gas among high energy users. Interest is increasing in the use of fuels generated through the gasification of fossil fuels (natural gas, coal, biomass, organic waste, etc.), which are known as syngas (synthetic gas), see, e.g., [1–3]. The search for financial and environmental benefits may also allow profit from unreacted fuel (known as off-gas) from fuel cell stacks (SOFC and MCFC), see, e.g., [4].

Studies have been made on the combustion characteristics of H_2/CO-rich fuels due to its importance in several applications [5–7]. The interest in developing combined heat and power (CHP) systems using SOFC has increased the relevance of the study on off-gas combustion technologies [8,9]. The syngas and off-gas combustion technologies deal with very lean fuel mixtures that are relevant for the gas turbines operation in internal gasification combined cycles (IGCC) and SOFC-GT hybrid systems [10].

Pure CO is difficult to burn because of the absence of chain carriers and chain branching reactions that are essential for flame propagation. However, the CO combustion rate can be enhanced by the addition of small amounts of H_2 or H_2O, see, e.g., [11]. The addition of H_2 to a fuel affects the physical nature of the flame and the flame stability. Consequently, the lean blow-out limit of a gas turbine combustor may be extended to lower equivalence ratios but also increases the risk of flashback [12]. Most of the H_2/CO mixtures contain also N_2, CO_2, H_2O, CH_4 and other species, and its H_2/CO volumetric

☆The support from EU under project FlameSOFC is gratefully acknowledged. M.A.A. Mendes and J.M.C. Pereira acknowledge the fellowships received from Fundação para a Ciência e a Tecnologia—FCT.

*Corresponding author.
E-mail address: jcfpereira@ist.utl.pt (J.C.F. Pereira).

0360-3199/$ - see front matter © 2008 International Association for Hydrogen Energy. Published by Elsevier Ltd. All rights reserved.
doi:10.1016/j.ijhydene.2008.04.019

Nomenclature

A	Arrhenius pre-exponential factor
a	concentration dependence of O_2 species in reaction 1
a_s	volumetric surface area
b	concentration dependence of H_2O species in reaction 2
c	concentration dependence of O_2 species in reaction 2
C_p	specific heat capacity
D	diffusion coefficient
E	activation energy
h	specific enthalpy
H_s	surface heat transfer coefficient
H_v	volumetric heat transfer coefficient
I	radiation intensity
L	length
MW	molecular weight
Q_r	radiative flux
R	universal gas constant, reaction rate
S_L	burning velocity
T	temperature
t	time
u	velocity
x	position
Y_k	mass fraction of species k in the gas mixture

Greek symbols

α_{kj}	stoichiometric coefficient for species k in reaction j
β	extinction coefficient
δ_k	species k perturbation amplitude
$\dot{\omega}$	chemical production rate
ε	solid emissivity
λ	thermal conductivity
μ	direction angle cosine
ω	scattering albedo
Φ	phase function
ϕ	solid porosity, equivalence ratio
ρ	density
σ	Stefan–Boltzmann constant
τ	optical depth, temperature perturbation amplitude
θ_j	eigenvalue associated with variable j

Superscript

$'$	perturbating quantity

Subscript

0	solid inlet
b	black body
cr	critical
f	flame
g	gas mixture
i	direction index
in	inlet gas mixture
k	species index
L	solid outlet
o	free flame
s	porous solid

ratio may vary from 0.33 to 40, as is the case of syngas, while the diluent gases are present with a fraction in between 4% to 51%, see, e.g., [1]. The very high disparity of H_2/CO volumetric ratio and diluent gases fraction may also be present in the off-gas from SOFC and MCFC fuel cells. When H_2 and CO are very diluted in inert species form a very lean mixture that is extremely difficult to burn in conventional free flame mode of operation, but it is potentially very attractive to be burned in inert porous media (IPM) burners. The premixed combustion of ultra-lean mixtures in IPM is one of the many advantages that IPM offers compared with free flames. The IPM combustion benefits from the higher heat recirculation provided by the solid matrix, see, e.g., [13–17]. Furthermore, the IPM combustion offers an increase of flame stability, high power modulation, a very compact burner design and low pollutant emissions if compared with free flames, see, e.g., [18–21]. The mechanism of heat recirculation in IPM transfers heat from the hot combustion products to preheat the unburned reactants, and can produce super-adiabatic temperatures which facilitate the combustion of ultra-rich and ultra-lean mixtures. Recent studies have focused on the IPM ultra-rich combustion to produce syngas [22,23].

The extinction, flashback and blow-off limits of lean methane–air surface flames were studied by Hanamura and Echigo [15]. They presented flame stabilization diagrams for submerged and surface flames and showed that for some values of equivalence ratio there is a flashback window in the velocity of surface flames. Tseng [24] studied the effect of H_2 addition to premixed combustion of methane in IPM, showing that the addition of H_2 to the fuel extends the ultra-lean flammability limit. The flame stabilization in IPM is important for burners operation and the variation of H_2/CO volumetric ratio is one of the problems that may affect them mostly. The combustion of these fuel mixtures in IPM can give rise to problems of flashback or blow-out. Therefore it is important to understand the effect of various parameters on H_2/CO flames within IPM to improve current IPM combustion systems. To the authors knowledge, the combustion of ultra-lean H_2/CO mixtures in IPM and its stability has not been reported, but their understanding benefits from the existing knowledge of the combustion of mixtures with sparse amounts of fuel, see, e.g., [24–26].

The objective of this study is to investigate the IPM flame stabilization mechanism of H_2/CO mixtures in the ultra-lean regime. The influence of several parameters (equivalence ratio, H_2/CO volumetric ratio, and reactants inlet temperature) on the IPM combustion performance and stability is analyzed. Flame stabilization diagrams are presented to provide useful

information, for the operation and safety of IPM burners, about the IPM flame stabilization mechanism of H_2/CO mixtures in the ultra-lean regime. Calculations of ultra-lean H_2/CO combustion in IPM are obtained with a one-dimensional numerical model. Linear stability analysis is performed to investigate the stability of the steady solutions as a function of burning velocity and flame location. The model solves the energy equations for the gas and solid phases accounting for the radiative heat transport in the solid. In order to make feasible the linear stability analysis, a global reaction model for the combustion of H_2 and CO and constant solid and gas properties were considered. Although it is expected that this simplified modeling approach cannot be used for quantitative predictions, it represents the main features of IPM combustion phenomena in a qualitative manner, see, e.g., [27,28], which is enough to satisfy the objectives of this study.

The modeling assumptions and governing equations of the process are given in the next section. This is followed by the predictions of the flame location in an idealized burner consisting of a short porous medium, made of SiC porous foam, inside a pipe. The linear stability analysis allowed to predict which of the flames are stable for several H_2/CO volumetric ratio and for two different inlet temperatures. The paper closes with the summary of conclusions.

2. Governing equations

The combustion of H_2/CO mixtures in IPM was simulated with a modified version of the PREMIX code [29,30] that incorporates the solid energy balance (including radiation) and the heat exchange between gas and solid phases. The numerical model constitutes a standard procedure for one-dimensional premixed combustion in porous media and was previously validated with excellent agreement against experimental temperature and concentration data [30] and also against other predictions [13].

We consider premixed laminar combustion of a ultra-lean H_2/CO–air mixture in a porous media of length L, see Fig. 1. We assume a one-dimensional geometry, inert homogeneous porous material made of a ceramic foam, constant pressure and negligible catalytic effects. With this assumptions the governing equations for mass, species and energy (of the gas and solid phases) are:

Continuity equation:

$$\frac{\partial(\phi\rho_g)}{\partial t}+\frac{\partial(\phi\rho_g u)}{\partial x}=0 \tag{1}$$

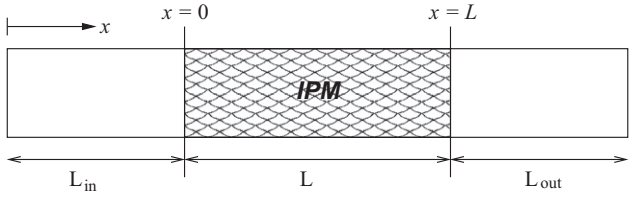

Fig. 1 – Computational domain ($L = 1.0$ cm; $L_{in} = L_{out} = 2.0$ cm).

Species transport equation:

$$\phi\rho_g\frac{\partial Y_k}{\partial t}+\phi\rho_g u\frac{\partial Y_k}{\partial x}-\frac{\partial}{\partial x}\left(\phi\rho_g D_k\frac{\partial Y_k}{\partial x}\right)-\phi\dot{\omega}_k MW_k=0 \tag{2}$$

Gas energy equation:

$$\begin{aligned}&\phi\rho_g C_{pg}\frac{\partial T_g}{\partial t}+\phi\rho_g u C_{pg}\frac{\partial T_g}{\partial x}-\frac{\partial}{\partial x}\left(\phi\lambda_g\frac{\partial T_g}{\partial x}\right)\\&-\phi\sum_k\rho_g C_{pk}D_k\frac{\partial Y_k}{\partial x}\frac{\partial T_g}{\partial x}+\phi\sum_k\dot{\omega}_k h_k MW_k\\&+H_v(T_g-T_s)=0\end{aligned} \tag{3}$$

Solid energy equation:

$$\begin{aligned}&\frac{\partial((1-\phi)\rho_s C_{ps}T_s)}{\partial t}-\frac{\partial}{\partial x}\left((1-\phi)\lambda_s\frac{\partial T_s}{\partial x}\right)\\&-H_v(T_g-T_s)+\frac{\partial Q_r}{\partial x}=0\end{aligned} \tag{4}$$

The porosity ϕ represents the volume fraction of the gas phase, therefore in regions outside the porous media ϕ equals 1 and Eq. (4) falls out, otherwise ϕ equals the solid porosity ϕ_s.

The boundaries of the computational domain were extended upstream and downstream of the foam, see Fig. 1, to ensure that the flames are not influenced by the inlet/outlet boundary conditions. It was assumed inlet Dirichlet conditions and outlet Neumann conditions for the mass, species and gas energy equations. The inlet/outlet boundary conditions for the solid energy equation are obtained by an energy balance at the surfaces of the foam:

$$x=0:\quad -\lambda_s\frac{\partial T_s}{\partial x}-H_s(T_g-T_s)+\varepsilon\sigma(T_s^4-T_0^4)=0 \tag{5}$$

$$x=L:\quad \lambda_s\frac{\partial T_s}{\partial x}-H_s(T_g-T_s)+\varepsilon\sigma(T_s^4-T_L^4)=0 \tag{6}$$

where $H_s=H_v/a_s$, $T_0=T_g|_{in}$, and $T_L=T_\infty$.

The interface conditions for the species and gas energy equations at the gas–solid interfaces are given in a similar way to ensure the continuity of fluxes [13]:

$$x=0:\quad \frac{\partial Y_k}{\partial x}|_-=\phi\frac{\partial Y_k}{\partial x}|_+ \tag{7}$$

$$\lambda_g\frac{\partial T_g}{\partial x}|_-+(1-\phi)H_s(T_g-T_s)=\phi\lambda_g\frac{\partial T_g}{\partial x}|_+ \tag{8}$$

$$x=L:\quad \phi\frac{\partial Y_k}{\partial x}|_-=\frac{\partial Y_k}{\partial x}|_+ \tag{9}$$

$$\phi\lambda_g\frac{\partial T_g}{\partial x}|_-+(1-\phi)H_s(T_g-T_s)=\lambda_g\frac{\partial T_g}{\partial x}|_+ \tag{10}$$

2.1. Chemical reaction modeling

The optimized detailed reaction mechanism for the oxidation of H_2/CO mixtures, presented in Davis et al. [31], allows good predictions for a wide range of inlet conditions. However, since the present study also involves the linearization of the governing equations for the linear stability study, it is not feasible with the detailed mechanism. Consequently, a simplified reaction mechanism has to be selected and a two-step global mechanism was used [32,33].

The oxidation of the H_2/CO fuel can be defined by the global two-step reaction mechanism:

$$\textit{reaction}\ 1:\quad H_2+\tfrac{1}{2}O_2\rightarrow H_2O \tag{11}$$

Table 1 – Reaction rate coefficients for the two-step mechanism

T_{in} (K)	$A_1\left(\frac{mol^{(-a)}}{cm^{-3a}\,s}\right)$	$\frac{E_1}{R}$ (K)	a	$A_2\left(\frac{mol^{(-b-c)}}{cm^{-3(b+c)}.s}\right)$	$\frac{E_2}{R}$ (K)	b	c
300	1.8×10^{13}	17 614.0	0.50	1.2×10^{11}	8053.0	0.30	0.50
500	3.0×10^{14}	18 335.0	0.53	4.8×10^{12}	12 100.0	0.29	0.52

$$\textit{reaction}\quad 2:\quad CO+\tfrac{1}{2}O_2\rightarrow CO_2 \tag{12}$$

with the respective reaction rates given in the Arrhenius form:

$$R_1 = A_1 e^{-E_1/RT_g}[H_2][O_2]^a \tag{13}$$

$$R_2 = A_2 e^{-E_2/RT_g}[CO][H_2O]^b[O_2]^c \tag{14}$$

and the species production rates appearing in Eqs. (2) and (3) are calculated by

$$\dot{\omega}_k = \sum_{j=1}^{2}\alpha_{kj}R_j \tag{15}$$

except for the N_2 species which is calculated from the total mass conservation of the gas mixture.

The reaction rate coefficients of Eqs. (13) and (14) are given in Table 1 for two different inlet mixture temperatures. The coefficient values for 300 K were taken from [32,33] and reasonable predictions of the burning velocity were obtained for H_2/CO ratios within the range 0.1–10. Since the model is very simplified these coefficients were adjusted to have satisfactory predictions at different inlet temperatures. For the inlet mixture temperature of 500 K the commercial optimization software ModeFRONTIER [34] was used to obtain optimized values of the reaction rate coefficients that reproduce the temperature and species evolution given by the detailed mechanism. This procedure allows to reduce the global model error in the burning velocity predictions and for the optimized range to obtain predictions close to the detailed mechanism for the specific case of interest.

2.2. Radiation modeling

For radiation purposes the porous material was considered as a diffuse, gray body together with a non-radiating gas mixture. The radiative heat source term $\partial Q_r/\partial x$ appearing in Eq. (4) is calculated from the one-dimensional radiative heat transfer equations [35]:

$$\mu\frac{dI}{d\tau} = (1-\omega)I_b - I + \frac{\omega}{2}\int_{-1}^{1} I(\tau,\mu_i)\Phi(\mu,\mu_i)\,d\mu_i \tag{16}$$

$$\frac{dQ_r}{d\tau} = (1-\omega)(4\pi I_b - 2\pi\int_{-1}^{1} I(\tau,\mu)\,d\mu) \tag{17}$$

with boundary conditions given by

$$I(\tau=0)=\frac{\sigma}{\pi}T_0^4$$
$$I(\tau=\beta L)=\frac{\sigma}{\pi}T_L^4 \tag{18}$$

where $\tau=\beta x$ is the optical depth and $I_b=\frac{\sigma}{\pi}T_s^4$, and assuming $T_0=T_{in}$ and $T_L=T_\infty$.

The system of Eqs. (16)–(18) was numerically solved using the discrete–ordinates method (S_2 approximation) [35].

2.3. Linear stability analysis

The development of instabilities in premixed combustion systems is commonly studied with linear stability analysis. The evolution of small disturbances in the system is assumed to be governed by the linearized form of Eqs. (1)–(4). The assumption of constant physical and transport properties for the solid and the gas mixture is required to successfully perform this linear stability analysis, and is commonly applied in linear stability studies conducted for flames [36–38]. Therefore, the variables of the problem were reduced to T_g, T_s, Y_k and u. There are two intrinsic instability mechanisms associated with premixed flames: the hydrodynamic instabilities related with velocity field perturbations and the diffuse-thermal instabilities related with thermal energy field perturbations [39]. Due to the one-dimensional character of this problem, the continuity Eq. (1) falls out of this analysis because, by assuming ρ_g constant, the velocity perturbation u' in the flow field velocity must be zero to satisfy continuity, and therefore the hydrodynamic instabilities are suppressed. This assumption appears to be restrictive, but previous studies showed that realistic qualitative results can be obtained [36–38]. It was also assumed that no perturbation exists on the inlet Dirichlet boundary conditions for the species and gas energy equations.

The linearized form of Eqs. (2)–(4), that describe small disturbances in the system, is obtained by the standard decomposition of the variables into a mean solution (T_g, T_s, Y_k) and a perturbation (T'_g, T'_s, Y'_k). Further, the mean part is subtracted from the rest, leaving just the perturbation terms, see, e.g., [36]. By applying the assumptions referred in the previous paragraph, the linearization of Eqs. (2)–(4) and respective boundary conditions gets trivial, except for the reaction rates R_1 and R_2 in Eqs. (2) and (3), and the radiation source term $\partial Q_r/\partial x$ appearing in Eq. (4). The reaction rate perturbations R'_1 and R'_2 are given by Eqs. (19) and (20), respectively, as explicit functions of T'_g and Y'_k:

$$R'_1 = \frac{A_1\rho^{(1+a)}e^{-E_1/RT_g}}{MW_{H_2}MW_{O_2}^a}\times\left[Y_{H_2}Y_{O_2}^a\frac{E_1}{R}\frac{T'_g}{T_g^2}+aY_{H_2}Y_{O_2}^{(a-1)}Y'_{O_2}+Y_{O_2}^aY'_{H_2}\right] \tag{19}$$

$$R'_2 = \frac{A_2\rho^{(1+b+c)}e^{-E_2/RT_g}}{MW_{CO}MW^b_{O_2}MW^c_{H_2O}}\left[Y_{CO}Y^b_{O_2}Y^c_{H_2O}\frac{E_2}{R}\frac{T'_g}{T^2_g} + bY_{CO}Y^{(1-b)}_{O_2}Y^c_{H_2O}Y'_{O_2} + cY_{CO}Y^b_{O_2}Y^{(c-1)}_{H_2O}Y'_{H_2O} + Y^b_{O_2}Y^c_{H_2O}Y'_{CO}\right] \quad (20)$$

The source term $\partial Q_r/\partial x$, in Eq. (4), is not trivial to linearize when the discrete–ordinates method is used to solve the one-dimensional radiative heat transfer Eqs. (16)–(18). To overcome this problem the following procedure was applied: firstly, by decomposing the radiative flux and the radiation intensity into a mean value (Q_r,I) and a perturbation (Q'_r,I'), Eqs. (16)–(18) were linearized; secondly, the S_2 approximation was applied to the resulting linear equations originating an ODE system; thirdly, its analytical solution was calculated using the software MATHEMATICA [40] yielding an integro-differential equation for the radiative flux term perturbation, which is given as an explicit function of the solid temperature perturbation T'_s as

$$\frac{\partial Q'_r}{\partial x} = (1-\omega)\beta(16\sigma T^3_s T'_s) - 2\pi\beta(1-\omega)\alpha(x)\left[\int_0^x a(t,x)T^3_s(t)T'_s(t)\,dt + \int_x^L b(t,x)T^3_s(t)T'_s(t)\,dt\right] \quad (21)$$

where

$$\alpha(x) = -\frac{6e^{-6\sqrt{5}x}}{5-3\sqrt{5}+(5+3\sqrt{5})e^{12\sqrt{5}}} \quad (22)$$

$$a(t,x) = \frac{1701}{250\,000}[(1+\sqrt{5})e^{12\sqrt{5}} - (\sqrt{5}-1)e^{12\sqrt{5}x}] \times[\cosh(6\sqrt{5}t) + \sqrt{5}\sinh(6\sqrt{5}t)] \quad (23)$$

$$b(t,x) = \frac{1701}{125\,000}e^{6\sqrt{5}(1+x)}[6\sqrt{5}\cosh(6\sqrt{5}(1-t+x)) - 2\cosh(6\sqrt{5}(-1+t+x)) + \sqrt{5}\sinh(6\sqrt{5}(1-t+x))] \quad (24)$$

for $L = 0.01$ m, $\beta = 1500.0\,m^{-1}$ and $\omega = 0.8$; finally, the resulting radiative flux term perturbation function (21) was introduced on the linearized equation for the solid energy perturbation, closing the linear perturbation equation system. The details of this procedure can be found in [41].

The set of linear equations that describe the small disturbances in the system accepts a nontrivial solution of the form (see, e.g., [36]):

$$Y'_k = \delta_k(x)e^{\theta_k t}$$
$$T'_g = \tau_g(x)e^{\theta_g t}$$
$$T'_s = \tau_s(x)e^{\theta_s t} \quad (25)$$

where the complex numbers $\theta_j\ j = k, g, s$ are the system eigenvalues. The system is said to be stable if the real part of θ, $\mathrm{Re}(\theta)<0$ for all θ, otherwise the small perturbations (25) will be amplified and the solution will be unstable.

After discretizing the perturbation equations of the system, a matrix eigenvalue problem was obtained. This matrix was solved to find the system eigenvalues which determine the stability condition of each steady solution. The real part of the system eigenvalues can be ordered as $\mathrm{Re}(\theta_1)>\mathrm{Re}(\theta_2)>\cdots$, where the highest value is the critical one ($\mathrm{Re}(\theta_1) = \mathrm{Re}(\theta_{cr})$) for the system stability condition.

3. Results

Firstly, the results are presented for the influence of three inlet mixture conditions (equivalence ratio (ϕ), H_2/CO volumetric ratio, and gas mixture inlet temperature (T_{in})) on the lean combustion of H_2/CO mixtures in IPM. Secondly, the linear stability analysis is presented for all the flames obtained. However, prior to the main results presentation, a discussion about the assumption of constant properties and global combustion model accuracy is required. Table 2 lists the values of the parameters and ceramic foam properties which were assumed to be constant. Due to the linear stability analysis, the gas mixture properties were assumed constant to avoid the inherent high complexity of perturbation fields of these properties. The present study assumes that the gas mixture properties (ρ_g, λ_g, D_k, C_{pg} and C_{pk}) are evaluated as the mean value between reactants and products of a free flame calculated with the specific inlet mixture parameters, and in this way the influence of these properties is not completely eliminated. In order to investigate the validity of this assumption several free flames were calculated and a comparison was made between the solutions obtained with constant and variable gas mixture properties. The two-step global reaction mechanism and the detailed mechanism of Davis et al. [31] were considered since the linear stability analysis is performed with the two-step global mechanism. The different inlet mixture conditions considered are listed in Table 3 where the values in bold highlight the changes from the reference case.

Fig. 2(a) shows the free flame burning velocity (S_{Lo}) as function of H_2/CO for various inlet mixture conditions, calculated with the detailed mechanism and variable gas

Table 2 – Parameter values used for all cases

ϕ_s	0.8	ρ_s	3.0×10^3 kg/m^3
H_v	2.0×10^6 W/(m^3 s)	C_{ps}	0.35 kJ/(kg K)
a_s	4000.0 m^{-1}	λ_s	0.8 W/(m K)
T_∞	300 K	β	1500.0 m^{-1}
ε	0.85	ω	0.8

Table 3 – Inlet mixture conditions used for the considered cases

Cases	H_2/CO	ϕ	T_{in} (K)
C_{ref}	**1**	**0.33**	**300**
C_A	**10**	0.33	300
C_B	1	**0.5**	300
C_C	1	0.33	**500**
C_D	**10**	0.33	**500**

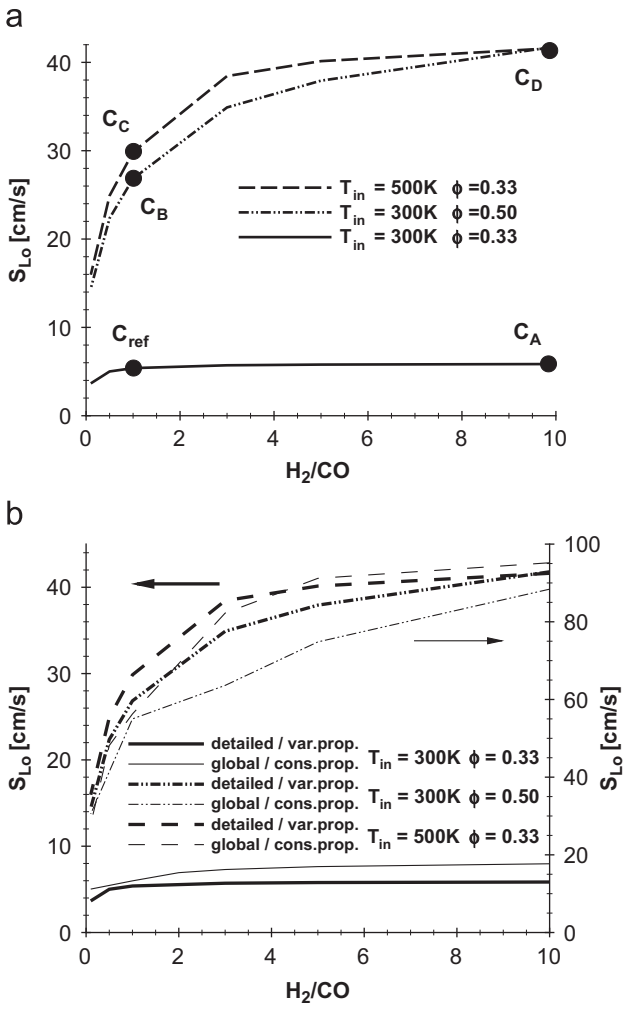

Fig. 2 – Free flame burning velocity as function of the volumetric H_2/CO ratio for various inlet mixture conditions: (a) S_L obtained with the detailed mechanism and variable gas properties; (b) comparison of the S_L value obtained with the two different modeling approaches (detailed mechanism/variable gas properties; global mechanism/ constant gas properties).

properties. It can be seen that the S_{Lo} value increases with H_2/CO and also with the T_{in} and ϕ increase. For lower inlet temperatures and leaner mixtures, Fig. 2(a) shows that the S_{Lo} value is very little sensitive to variations in H_2/CO.

Fig. 2(b) presents the comparison between the S_{Lo} values obtained with the two different modeling approaches for the different inlet mixture conditions. For all the cases, the qualitative evolution of S_{Lo} is similar for both modeling approaches, although the S_{Lo} value obtained with the global mechanism and constant gas mixture properties is greater than the value obtained with the detailed mechanism and variable properties. Therefore the simplified modeling approach can simulate the qualitative effect of different inlet mixture conditions on S_{Lo}, but obviously the detailed reaction mechanism with variable gas properties provides more accurate data.

The simplified modeling approach used in this study is sufficient to represent the main features of the premixed flame stabilization phenomena in IPM. An example of that is the comparison between the analytical study of Schoegl and Ellzey [28] and the numerical study of Lammers and de Goey [42]. In the first, a simple analytical one-dimensional model, applying activation energy asymptotics and constant solid and gas properties, is used to study the effect of several parameters (including equivalent ratio and inlet gas temperature) on the stabilization of premixed flames in IPM. In the second, a similar study is performed with numerical simulations, using an elaborated one-dimensional model including detailed chemistry and solid phase radiation, to understand the flashback phenomena of premixed flames in porous burners. Comparing the resulting temperature profiles and stabilization diagrams (burning velocity vs. flame location), it can be concluded that both modeling approaches lead to qualitatively similar results regarding both flame stabilization position and flame thickness.

3.1. *Results of steady solutions*

The reference conditions (named C_{ref}) correspond to an ultra-lean fuel-air mixture with H_2/CO volumetric ratio equal to unity, and inlet ambient temperature. From the reference case C_{ref} other cases were created to study the effect of varying the inlet mixture H_2/CO volumetric ratio, ϕ and T_{in} on the steady flame solutions within IPM, as listed in Table 3.

Figs. 3(a)–(c) show the results of ultra-lean H_2/CO mixture combustion within IPM corresponding to C_{ref} conditions. Fig. 3(a) presents a stabilization diagram with the dimensionless burning velocity S_L/S_{Lo} plotted as function of the flame front location x_f. The S_{Lo} value corresponds to the free flame burning velocity at C_{ref} conditions, and x_f is assumed to be located at the position where occurs the maximum heat release rate [14]. Fig. 3(a) shows that two distinct combustion modes are possible, corresponding to submerged and surface flames. No solutions exist on the gas/solid interfaces for this reference case. In the submerged flame mode some flame zones can show S_L values much higher than S_{Lo} due to heat recirculation, but surface flames only present S_L values lower than S_{Lo}.

Either submerged or surface flames may have, at the same location, two completely different solutions characterized by different burning velocities and temperature profiles. These two different flames, existing at the same location, correspond to the upper and lower solution branches. Both types of flames exist in practical burners and stable or oscillatory operation may result [43–45], being that for some zones the combustion process can be unstable. Figs. 3(b) and (c) give examples of temperature and heat release rate profiles for the upper and lower branches. The lower branch flames present a very thick reaction zone with sub-adiabatic flame temperatures almost in equilibrium with the solid, while the upper flames have thinner reaction zones and can present super-adiabatic peak temperatures. For submerged flames, there is also the possibility to have two flames with the same burning velocity value but located at different positions, corresponding to the intersection points of the closed curve of Fig. 3(a) with lines parallel to *x*-axis.

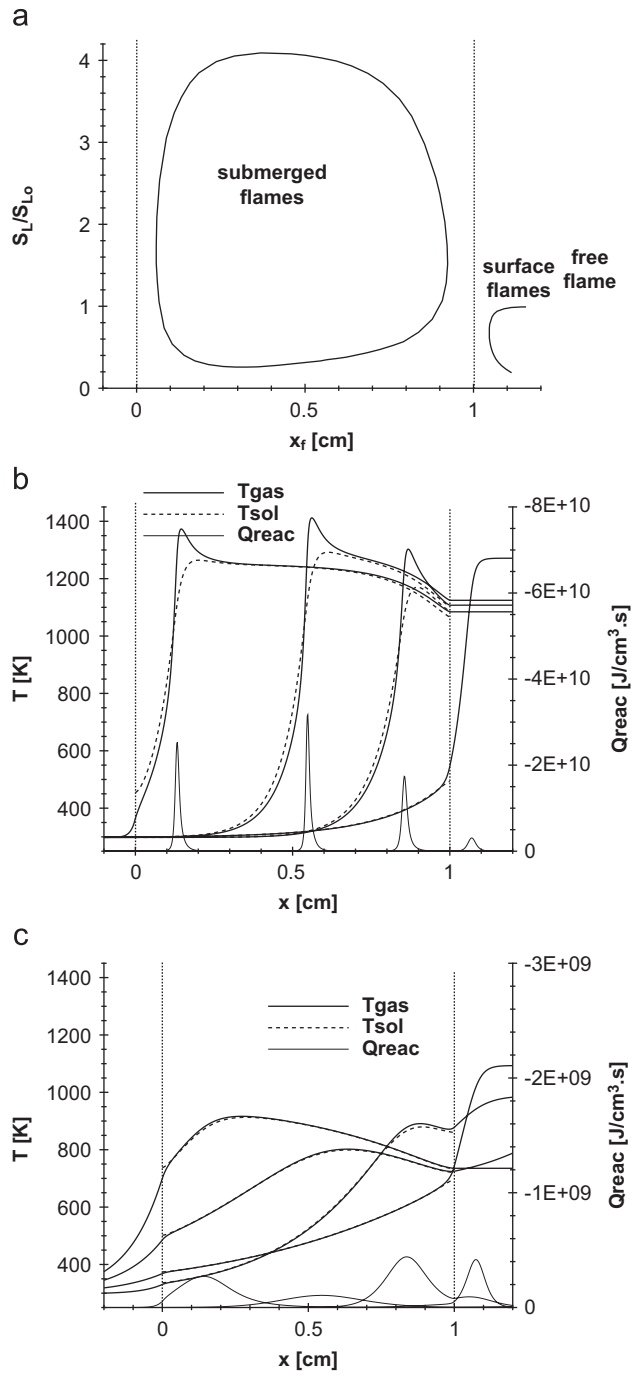

Fig. 3 – IPM combustion of H_2/CO mixture at case C_{ref} conditions: (a) stabilization diagram; (b) gas and solid temperature and heat release rate profiles for upper branch flames and (c) gas and solid temperature and heat release rate profiles for lower branch flames.

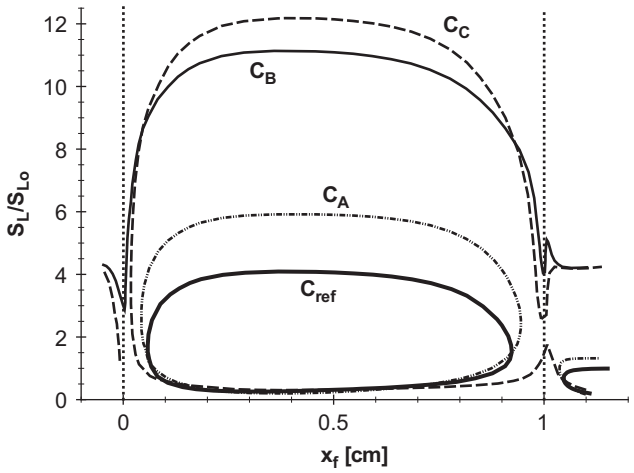

Fig. 4 – Effect of the inlet H_2/CO mixture conditions (H_2/CO, ϕ and T_{in}) on the IPM combustion characteristics.

Fig. 4 shows the normalized burning velocity as a function of flame position for the first four inlet mixture conditions listed in Table 3. Fig. 4 also shows that the increase of the H_2/CO volumetric ratio, from unity (case C_{ref}) to 10 (case C_A), keeping the same ϕ and inlet temperature, has a relative small influence producing only a slight increase of the immersed upper solutions burning velocity. When the equivalence ratio (case C_B) or the inlet temperature (case C_C) is increased in comparison with C_{ref}, large differences are obtained in the burning velocity and mainly in the flame location. Cases C_B and C_C have originated the existence of steady solutions at the gas/solid interfaces, but also create a gap window on the S_L value where no steady solutions exist. This originates the flashback of submerged and surface flames and is of practical importance for the project of IPM burners, see, e.g., [42]. From the case C_C it can be concluded that this flashback window tends to appear first at the outlet interface affecting the downstream surface flames. Fig. 4 shows that, when the surface flames touch the outlet gas/solid interface, there is the creation of the flashback window, and it also appears a peak on the burning velocity. This originates three different upper solutions in the vicinity of the outlet surface of the burner (one submerged and two surface flames) as it is seen in case C_B. This phenomena was not observed close to the burner inlet surface.

3.2. *Results of the linear stability analysis*

In the previous section the impact of several inlet mixture conditions on the H_2/CO flame stabilization mechanism was investigated, and the solutions corresponding to the flame locations were predicted. Questions arise if these flames are stable or unstable and to clarify this issue a discussion about the linear stability of these flames is presented in this section.

We have applied the linear stability analysis also to free flames and the predictions show that the increase of the H_2 concentration in the reactants mixture increases the flame stability. It is known that CO-rich mixtures are difficult to burn and that the addition of small amounts of H_2 helps to the flame stabilization, by increasing the CO combustion rate [11]. Therefore, the model predictions and the linear stability analysis seem to be in qualitative agreement with previous studies. The numerical study of Tseng [24] shows that the addition of H_2 to the reactants extends the lean limit of methane/air flames, increasing the flame stability. In

addition, it was observed that, for different inlet mixture conditions, the H_2/CO free flames become unstable ($Re(\theta_{cr})>0$) for H_2/CO volumetric ratios below a certain critical value, which was found to lay between 1 and 2. This critical H_2/CO ratio seems to be excessively high, probably due to the model simplicity, but to the authors knowledge no experimental results exist to clarify this prediction. From the comparison of the real part of the highest eigenvalue ($Re(\theta_{cr})$) of the system, it can be concluded that higher inlet mixture temperatures and richer mixtures increase the flame stability, as shown in Fig. 5. The $Re(\theta_{cr})$ behavior also shows that the flame stability increases with H_2/CO.

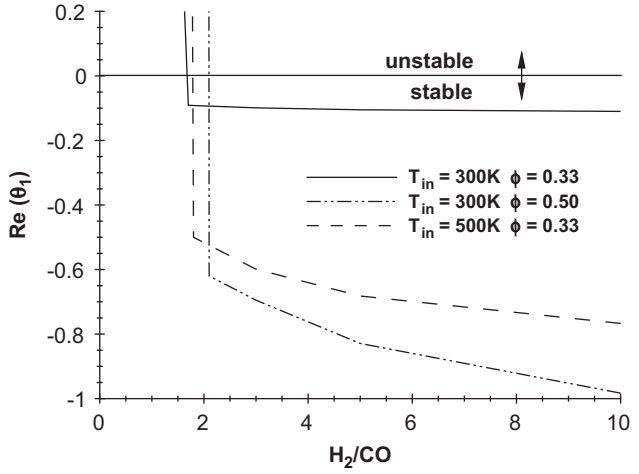

Fig. 5 – Highest (critical) eigenvalue of the free flame system ($Re(\theta_{cr})$) as function of the volumetric H_2/CO ratio for various inlet mixture conditions.

Fig. 6 presents the stabilization diagrams of the IPM flame solutions obtained for the different inlet conditions listed in Table 3 with the results from the linear stability analysis. The stable and unstable flame regions are made distinct by continuous or dashed lines, respectively. It has been suggested by Buckmaster and Takeno [27] that the solutions in the stabilization diagram must lay upon segments with positive slope ($\partial S_L/\partial x_f>0$) for the flame to be stable. This stability condition was found to work just for the upper branch of surface flames. However, the same was not observed for the upper branch of submerged flames, due to the solid radiation which increases flame stability, shifting the stable–unstable transition to regions where $(\partial S_L/\partial S_{Lo})/\partial x_f$ is negative. For the lower branch solutions (submerged and surface flames) the flame stability also depends on the S_L slope, but stable flames were found in regions with negative slope ($\partial S_L/\partial x_f<0$).

It can be concluded from the reference case C_{ref} that it is possible to have stable submerged and surface flames with IPM combustion, although the present linear stability analysis gives an unstable free flame behavior. The surface flames existing closer to the outlet surface of the porous burner are found to be stable, as well as the submerged flames on the

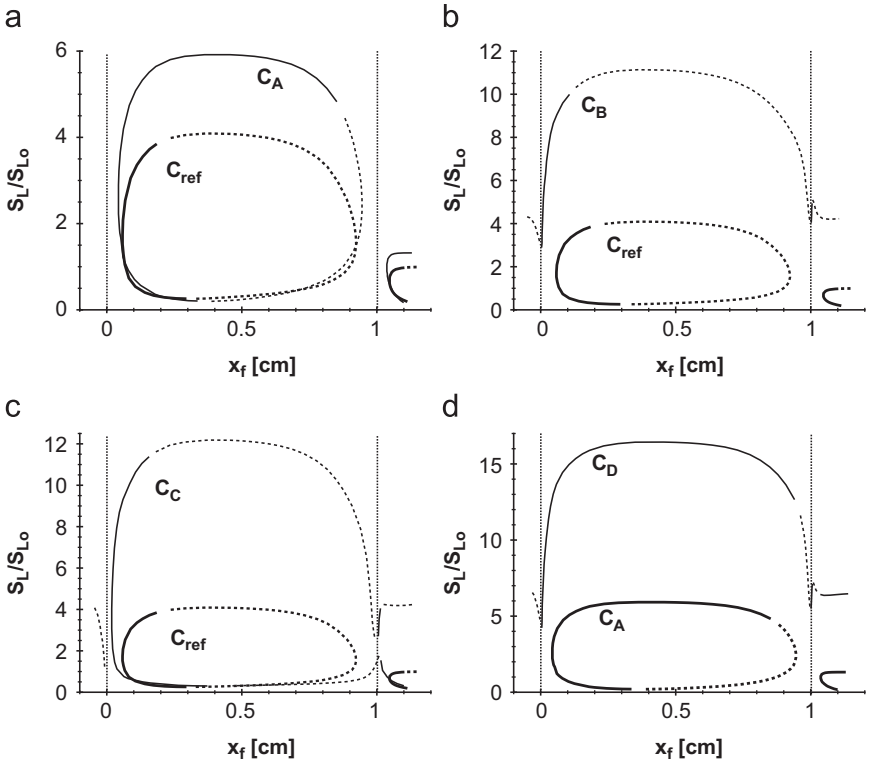

Fig. 6 – Stabilization diagrams with the impact of the inlet H_2/CO mixture conditions on linear stability analysis of the IPM combustion: variation of (a) H_2/CO; (b) ϕ; (c) T_{in} and (d) H_2/CO and T_{in} (solid lines are stable solutions and dashed lines are unstable).

upstream part of the burner. Therefore, the IPM combustion promotes the ultra-lean burning of H_2/CO mixtures.

Fig. 6(a) shows the impact of H_2/CO volumetric ratio on the flame stability for an ultra-lean mixture at low inlet temperature. It is observed that the increase of H_2/CO volumetric ratio extends the stable flame regions, and all the surface flames of case C_A are made stable. For the upper branch of the submerged flames the stable region is extended in the downstream region, where S_L presents a negative slope. This shows that the increasing of H_2 in the mixture has a positive effect on the IPM flame stability.

The effect of the equivalence ratio and the inlet mixture temperature on the flame stability is shown in Figs. 6(b) and (c), respectively. For the present cases where H_2/CO volumetric ratio equals unity, the increase of ϕ and T_{in} has a negligible influence on the extension of the stable submerged flame region. This can be explained by the linear stability results, which give unstable free flames for low H_2/CO volumetric ratios (including cases C_{ref}, C_B and C_C), see Fig. 5. However, for higher H_2/CO volumetric ratios, where the free flames were found to be stable, the increase of ϕ and T_{in} extends the stable submerged flame region. This is shown in Fig. 6(d), for the increase of T_{in}, comparing cases C_A and C_D which have $H_2/CO = 10$. A similar effect is obtained for the increase of ϕ (not shown here). It must be noted that the increase of ϕ and T_{in} also creates a gap window on the velocity which increases the danger of flashback on the stable submerged and surface flames close to the boundaries of the porous burner.

For an ultra-lean mixture entering the IPM at a high inlet temperature the increase of H_2/CO volumetric ratio also extends the stable flame regions, but promotes the emergence of the flashback window on the flame velocity. This can be seen by comparing cases C_C and C_D in Figs. 6(c) and (d), respectively. The same was not observed at a low inlet temperature, see cases C_{ref} and C_A in Fig. 6(a). This phenomena can be related with [12], in which the high temperature combustion of syngas in gas turbines is studied, and states that increasing the concentration of H_2 in the fuel extends the lean blow-off limit, and also increases the risk of flashback.

4. Conclusions

A numerical simulation was performed on the premixed combustion of H_2/CO mixtures in inert porous media. The numerical model comprises one-dimensional energy equations for gas and solid phases and a rigorous treatment for radiative heat transfer together with a simplified reaction kinetics (two-step global mechanism and constant properties). Nevertheless, it was shown by comparison with a detailed reaction mechanism, that the model can simulate qualitatively the effect of different inlet mixture conditions on the burning velocity. The simplified mechanism was used to make possible the linear stability analysis.

Several IPM flames with different H_2/CO mixtures were analyzed, corresponding to combinations of H_2/CO volumetric ratio (1 and 10), inlet mixture temperature (300 and 500 K), and equivalence ratio (0.33 and 0.5). Based on the results, the following conclusions can be drawn:

(i) Increase of the H_2/CO volumetric ratio, from 1 to 10, has a relative small influence in the ultra-lean regime, at low temperatures, producing only a slight increase of the immersed upper solution burning velocity and extending the stable submerged flame region. At higher inlet temperatures, the increase of the H_2/CO volumetric ratio not only promotes the emergence of a gap window on the S_L value, where no steady solutions exist, but also extends the stable submerged flame region.

(ii) For high H_2/CO volumetric ratios, the increase of the equivalence ratio and inlet temperature slightly extends the stable submerged flame region, but this effect is reduced for lower H_2/CO volumetric ratios.

(iii) Increase of the equivalence ratio or the inlet temperature produces a large difference in the burning velocity and mainly in the flame location. It originates steady solutions at the gas/solid interfaces, but also creates a gap window on the S_L value where no steady solutions exist. This gap window tends to appear first at the outlet interface for ultra-lean mixture with low H_2/CO volumetric ratio, affecting the surface flames. Moreover, the emergence of the gap window on the velocity increases the danger of flashback on the stable submerged and surface flames close to the boundaries of the porous burner.

(iv) From the linear stability results it can be concluded that the IPM combustion promotes the ultra-lean burning of H_2/CO mixtures.

REFERENCES

[1] Moliere M. ASME paper #02-GT-30017; 2002.
[2] Minchener AJ. Fuel 2005;84:2222–35.
[3] Morris M, Waldheim L. Waste Manage 1998;18:557–64.
[4] Larminie J, Dicks A. Fuel cell systems explained. England: Wiley; 2003.
[5] Cuoci A, et al. Int J Hydrogen Energy 2007;32:3486–500.
[6] Natarajan J, et al. Combust Flame 2007;151:104–19.
[7] Som S, et al. Fuel 2007; in press.
[8] University of Cambridge, Combustion research fuel cell off-gas combustor ⟨http://www-diva.eng.cam.ac.uk/energy/combustion/off_gas.html⟩.
[9] FLAME-SOFC, EU project no. 019875 ⟨http://www.flamesofc.org/public/⟩.
[10] de Biasi V. Gas Turbine World 2005;35:28–30.
[11] Turns SR. An introduction to combustion: concepts and applications. 2nd ed. New York: McGraw-Hill; 2000.
[12] Drnevich R, et al., Praxair final report DE-FC26-03NT41892; 2004.
[13] Diamantis DJ, et al. Combust Theory Modelling 2002;6:383–411.
[14] Barra AJ, Ellzey JL. Combust Flame 2004;137:230–41.
[15] Hanamura K, Echigo R. Warme und Stoffubertragung 1991;26:377–83.
[16] Sathe SB, Tong TW. J Heat Transfer 1991;113:423–8.
[17] Yoshizawa Y, et al. Int J Heat Mass Transfer 1988;31:311–9.
[18] Brenner G, et al. Combust Flame 2000;123:201–13.
[19] Mößbauer S, et al. In: 5th international conference on technologies and combustion for a clean environment, Lisbon; 1999. p. 519–23.
[20] Howell JR, et al. Prog Energy Combust Sci 1996;22:121–45.

[21] Oliveira AAM, Kaviany N. Prog Energy Combust Sci 2001;27:523–45.
[22] Pedersen-Mjaanes H, et al. Int J Hydrogen Energy 2005;30:579–92.
[23] Dhamrat RS, Ellzey JL. Combust Flame 2006;144:698–709.
[24] Tseng C. Int J Hydrogen Energy 2002;27:699–707.
[25] Henneke MR, Ellzey JL. Combust Flame 1999;117:832–40.
[26] Kennedy LA, et al. Int Symp Combust 2000;28:1431–8.
[27] Buckmaster J, Takeno T. Combust Sci Technol 1981;25:153–8.
[28] Schoegl I, Ellzey JL. Combust Flame 2007;151:142–59.
[29] Kee RJ, Grcar JF, Smooke MD, Miller JA. A Fortran program for modeling steady laminar one-dimensional premixed flames, Report SAND85-8240, Sandia National Laboratories; 1996.
[30] Zhou XY, Pereira JCP. Fire Mater 1998;22:187–97.
[31] Davis SG, et al. Proc Combust Inst 2005;30:1283–92.
[32] Howard JB, et al. In: 14th international symposium on combustion, vol. 28; 1972. p. 975–86.
[33] Marinov NM, et al. In: 8th international symposium on transport properties, San Francisco, CA; 1995.
[34] ModeFRONTIER, Home page ⟨http://network.modefrontier.-eu/index.html⟩.
[35] Modest MF. Radiative heat transfer. New York: McGraw-Hill; 1993.
[36] Vance R, et al. Combust Theory Modelling 2001;5:147–61.
[37] Kurdyumov VN, Matalon M. Combust Flame 2008;153:105–18.
[38] Chao BH. Combust Flame 2001;126:1476–88.
[39] Yuan J, Ju Y, Law CK. Combust Flame 2006;144:386–97.
[40] Wolfram Research, Inc. Mathematica—version 5.2. Champaign, Illinois: Wolfram Research, Inc., 2005.
[41] Mendes MAA, Pereira JMC, Pereira JCF. Combust Flame 2008; in press, doi:10.1016/j.combustflame.2008.03.010.
[42] Lammers FA, de Goey LPH. Combust Flame 2003;133:47–61.
[43] Vogel BJ, Ellzey JL. Combust Sci Technol 2005;177:1323–38.
[44] Min DK, Shin HD. Int J Heat Mass Transfer 1991;34:341–56.
[45] Lee YI, et al. Combust Sci Technol 1996;112:75–93.